Nordic Hydrology, 24, 1993, 95-110

Numerical Modelling of Phase Change in Freezing and Thawing Unsaturated Soil

Paper presented at the 9th Northern Res. Basin Symposium/Workshop
(Whitehorse/Dawson/Inuvik, Canada – August 1992)

H. Engelmark and U. Svensson

Luleå University of Technology, S-951 87, Sweden

This paper presents a new method for handling the phase change process in numerical simultations of freezing and thawing soils. Moisture and heat transfer in soils subjected to both freezing and thawing are discussed. Simulated freezing results of temperature and total water content (water + ice) are compared with experimental data reported by Jame (1977). Simulated and experimental results were similar. The effects of different time-dependent temperature boundary conditions were evaluated and discussed. The method was used both with abrupt and smooth temperature boundary conditions and both resulted in stable numerical solutions. Finally, results from a simulation of a freezing and thawing cycle are presented and discussed qualitatively.

Introduction

Problems associated with seasonal freezing and thawing processes occur in natural and man modified soil environments. To optimize various technical solutions in such areas the importance of accurately predicting heat and water flow in seasonally freezing and thawing soils is obvious.

A phase change between water and ice occurs in moist soils subjected to freezing and thawing. In concentrating on water transport phenomena in frozen soil, it can be demonstrated that the heat and moisture flow relationships are coupled to relationships for mass balance and phase change. In such "hydraulic" models, ice is

characterized as it was air, *i.e.* ice pressure is assumed to be zero. An essential part of the coupling is a relationship between unfrozen water content and freezing temperatures, defined as SWFC (soil-water-freezing-characteristic).

Numerical models based on the hydraulic method and SWFC have been presented by a number of authors including Harlan (1973), Guymon and Luthin (1974), Jame (1977), Jame and Norum (1980), Motovilov (1977), Sheppard *et al.* (1978), Taylor and Luthin (1978), Guymon *et al.* (1980), Jansson and Halldin (1980) (see also Halldin *et al.* 1980), Hromadka *et al.* (1981), Engelmark (1984, 1986), Kung and Steenhuis (1986), Cary (1987) and Karvonen (1988, 1989).

In the models listed above, the heat and moisture transfer in the frozen zone were solved either separately or combined into a single equation. The degree of simplification differed between the models. The phase change or the ice-component calculations were usually performed using different iterative numerical procedures.

The objective of this paper is to present a new numerical method for handling the phase change process. The authors consider the physical interpretation of the method to be easier, than most of the models referred to above. In the new method, heat and mass transfer equations for soils subjected to both freezing and thawing (but without heaving and transport of mass in the air phase), are solved numerically. This new method for handling the phase change process is based on a total energy balance together with SWFC. The total energy balance of the frozen zone includes sensible and latent heat components. The phase change during a time increment is calculated, without any iteration, after the heat and water flow equations are solved for the same time increment (*i.e.* a two-step approach).

Mathematical Formulation

Basic Equations

Moisture transfer in the frozen unsaturated subsurface soil is described by the diffusion form of the mass conservation equation

$$\frac{\partial \theta_w}{\partial t} + \frac{\rho_I}{\rho}\frac{\partial \theta_I}{\partial t} = \frac{\partial}{\partial z}\left(D\frac{\partial \theta_w}{\partial z}\right) + \frac{\partial K}{\partial z} \qquad (1)$$

where θ_w and θ_I are unfrozen water content and ice content, (by volume of total soil volume). Water and ice densities (kg/m^3) are denoted ϱ and ϱ_I, respectively. K is the hydraulic conductivity (m/s), t is time (s), z is space coordinate (m) and D is the diffusivity coefficient (m^2/s) as defined by Childs and Collis-George (1950)

$$D = K\frac{\partial \psi}{\partial \theta_w} \qquad (2)$$

where ψ is the pore water pressure (m).

The heat transfer, neglecting heat associated with convective water flow (*e.g.* Taylor and Luthin 1976), can be expressed as follows (Halldin *et al.* 1980)

$$\frac{\partial C_m T}{\partial t} - L\frac{\rho_I}{\rho}\frac{\partial \theta_I}{\partial t} \equiv \frac{\partial}{\partial z}\left(K_T \frac{\partial T}{\partial z}\right) \qquad (3)$$

where C_m is the volumetric heat capacity (J/m^3 °C) and K_T is thermal conductivity (J/sm°C) in the soil-ice-water system. L is volumetric latent heat of fusion of liquid water (J/m^3) and T is temperature (°C).

Only partial freezing of the water content of the soil occurs when the temperature drops below 0°C. Measurements in a fine sandy loam by Ayers and Campbell (1951), for example, showed that the unfrozen water content decreased exponentially from about 17 % at −0.1°C to about 6 %, by volume, at −1.3°C. This SWFC is usually expressed by an equation of the form

$$\theta_w \equiv \theta_w(T) \quad , \qquad T<0^{\circ}C \qquad (4)$$

The particular form of $\theta_w(T)$ depends on the type of soil considered. Jame (1972) experimentally found that the shape of the curve describing the unfrozen water content function, $\theta_w(T)$ was independent of the initial water content.

Proposed Method of Solution

It is assumed that an expression for the diffusivity, D, is given. Two equations, Eq. (1) and Eq. (3), and one empirical relation Eq. (4) are available for solving the three unknown variables θ_w, θ_I and T. The main steps in the method are as follows.

I) Solve Eq. (1) and Eq. (3) neglecting changes in ice content, *i.e.* $\partial\theta_I/\partial t = 0$.
II) Adjust T, θ_w and θ_I using the empirical relation Eq. (4) and a constraint given by conservation of sensible and latent heat components. Note that transport effects are not considered in this step.

Step I is straightforward because the time derivative of the dependent variable is part of Eqs. (1) and (3). Step II is used when $T \leqslant 0$°C and/or when $\theta_I > 0$ and requires further consideration.

Eq. (4) is described here by a number of linear equations of the form

$$T_2 = r_1 \theta_{w_2} + r_0 \qquad (5)$$

where r_0 and r_1 are intersection and slope coefficients.

Eq. (5) is schematically shown in Fig. 1. Before step I is performed, the solution is in equilibrium at a position 0, Fig. 1. After step I, new values for θ_w and T are obtained, and these are denoted by position 1 in Fig. 1. Note that in step I, Eqs. (1) and (3) are discretized in terms of θ_{w_1} and $(C_m T)_1$ of the adjacent nodes, respectively.

In the second step II, position 1 in Fig. 1 is to be brought back to the straight line at position 2, which requires adjustments of $\Delta\theta_w$ and ΔT. The following relations

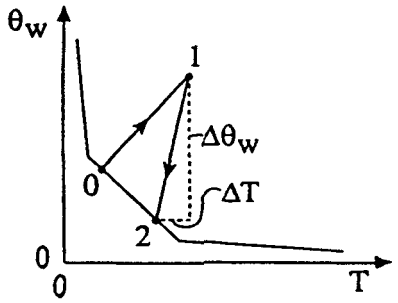

Fig. 1.
Schematic representation of unfrozen water content versus temperature < 0°C, SWFC.

be formulated

$$T_2 = T_1 + \Delta T \tag{6}$$

$$\theta_{w_2} \equiv \theta_{w_1} + \Delta\theta_w \tag{7}$$

Finally, energy conservation requires

$$\theta_s \rho_s c_s T_1 + \theta_{w_1} \rho c_w T_1 + \theta_{I_0} \rho_I c_I T_1 - L\theta_{I_0} \frac{\rho_I}{\rho} = \theta_s \rho_s c_s (T_1+\Delta T) +$$

$$(\theta_{w_1}+\Delta\theta_w)\rho c_w (T_1+\Delta T) + (\theta_{I_0}-\Delta\theta_w \frac{\rho}{\rho_I})\rho_I c_I (T_1+\Delta T) - L(\theta_{I_0} \frac{\rho_I}{\rho} - \Delta\theta_w) \tag{8}$$

where θ_s is volumetric soil content; ϱ_s is soil compact density (kg/m^3); and c_s, c_w and c_I are heat capacities of soil, water and ice (J/kg°C), respectively. The change in water/ice content, is denoted by $\Delta\theta_w$. ΔT, is the corresponding increase/decrease of temperature due to freezing/melting, respectively.

Reducing and rearranging Eq. (8) gives

$$\Delta T \equiv \Delta\theta_w \frac{(T_1\rho(c_I-c_w)-L)}{(C_m-\Delta\theta_w\rho(c_I-c_w))} \tag{9}$$

where

$$C_m \equiv \theta_s \rho_s c_s + \theta_{w_1} \rho c_w + \theta_{I_0} \rho_I c_I$$

Eqs. (5), (6), (7) and (9) give $\Delta\theta_w$ and ΔT and hence θ_{w2} and T_2. When $\Delta\theta_w$ is obtained, $\Delta\theta_I$ (from position 0 to 2) can also be determined because the total content of ice and water does not change during step II.

Numerical Solution

The set of equations formulated was solved by PROBE (Svensson 1986). PROBE is based on the finite-volume technique and employs a fully implicit numerical scheme. The number of grid cells in the calculations was about 300 and the time-

step was about 1 second. The regions of high non-linearity, *i.e.* at the frost and melt fronts, and the simulation accuracy of the moisture migration caused the small space and time increments. Regarding time and space resolution in the finite-volume technique, see for example Jensen (1983). In each validation solution, grid-independence in space and time was assured, therefore the numerical solution represented the true implication of the mathematical model.

Results

Validation

Validation of the model with the suggested solution for phase-change effects was performed using measured data from laboratory freezing experiments by Jame (1977). In these experiments, silica sand (dry density; 1,335 kg/m^3, porosity; 0.49) was used in 0.30 m long horizontal columns with uniform initial temperatures and soil water contents. Hollow brass liquid circulation plates were placed at both ends of the column. The unit was sealed with wax so that no water could flow into or out of the system. Provision was made for air movement so that the air within the column remained at atmospheric pressure. One end of the columns was exposed to a temperature below 0°C while at the other end a constant temperature above 0°C was maintained. Temperatures and soil water contents were monitored for periods of up to 72 hours. Soil heaving and ice lens formation was not observed. Details of soil and other relevant parameters from that study have been formulated in equations for direct use in numerical models (Engelmark 1992).

Three of the experiments reported by Jame (1977) were simulated using the model, and compared with measured data. The initial moisture contents were 15.00, 10.08 and 15.59 % by dry weight and the initial soil and warm end temperatures were +4.5, +5.0, +20.0°C, respectively. Corresponding cold end temperatures were −5.9, −5.3 and −10.0°C, respectively. Since the initial temperature profiles of the two first tests were not completely uniform, the measured data were used in the calculations. Note that in the validation of the model as applied to these horizontal freezing experiments, the hydraulic conductivity gradient, $\partial K/\partial z$, of Eq. (1) was zero.

Boundary conditions in the calculations are $\partial\theta_w/\partial z = 0$; $t \geq 0$, $z = 0$ and $z = L$, $T = T_c$; $z = 0$ and $T = T_w$; $z = L$, where T_c and T_w are temperatures at the ends of the soil column and may be time-dependent. Space coordinates and time are denoted by z and t, respectively. The *initial conditions* are $T = T_0$, $\theta_I = (\theta_I)_0$, $\theta_w = (\theta_w)_0$; $0 \leqslant z \leqslant L$ and $t = 0$, where T_0, $(\theta_I)_0$ and $(\theta_w)_0$ are known values of temperature, ice and water contents, respectively. These values can either be constant or functions of z.

Results of experimental and simulated data are shown in Figs. 2-4. Experimental data on moisture contents were plotted about 0.01 m apart, though the measured

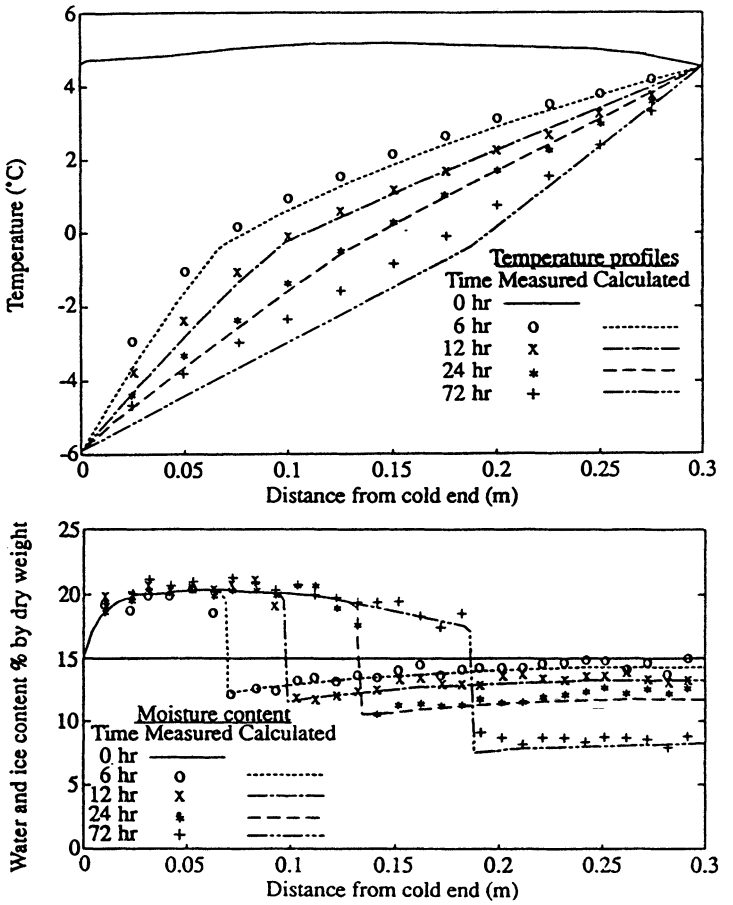

Fig. 2. Experimental data from Jame (1977) and simulation results of test 1, showing temperature and moisture content profiles.

points (*e.g.* Jame and Norum 1980) were not as strictly positioned. The reproduction errors were however, usually less than ± 0.002 m along the horizontal axes in Figs. 2-4.

Simulated temperature and moisture content profiles from *test 1*, during a period up to 72 hours, are shown in Fig. 2. The temperature gradient was approximately 34°C/m in the column.

Discrepancies between measured and calculated temperatures were evident, particularly at 6 and 72 hours, where deviations of up to 0.7°C occurred. These discrepancies indicated that the boundary condition may be was too strong. According to Jame (1977), the applied boundary temperature at the cold end during the experiment could not be measured as a one-step change of temperature at the cold end of the soil column. A smooth time-temperature boundary condi-

tion, based on measured soil temperature at the cold end of the column, decreased however the discrepancies only near the start of the experiment. Calculated temperatures at 6 hours were 0.3°C lower than measured at $z = 0.025$ m and for $z \geqslant 0.075$ m, the discrepancies were less than 0.15°C. At 72 hours, the temperatures were identical to those in Fig. 2 for $z > 0.075$ m. Measured temperatures in the soil profile at 72 hours, reported by Jame (1977), indicated that his reported applied temperature of −5.9°C at the cold end was too low.

Fig. 2 shows that the simulated moisture profiles followed the measured moisture profiles closely. For example, each calculated frost front position was located within the distance between the two adjacent measurement positions that covered each measured frost front. The abrupt boundary condition at the cold end strongly affected the curve describing the total moisture content within 0-0.01 m of the cold end. In this region no measurement of moisture content existed. However, according to Jame (1977), no ice layer was found directly under the cold plate at the end of each test. This suggests that no extremely high moisture content was accumulated at the cold end.

The simulation of test 1 with the smooth time-temperature boundary condition showed on the other hand, that the total moisture content was about 20 % at the cold end boundary. This moisture content was similar to the amounts of adjacent measured values. At a distance of about 10 mm from the cold end however, the moisture profiles were the same as the results presented in Fig. 2, except for the frost fronts near the start of the test period. The frost fronts were defined as the zones (positions) where water transforms into ice, *i.e.* the vertical sections of the total moisture content curves in Figs. 2-4. The difference in frost front position due to different temperature boundary conditions was however only 5 mm at 6 hours, and then decreased with time.

According to Jame (1977), some difficulties were encountered in simulating the temperature conditions at the cold end. In an effort to avoid these difficulties, he used the measured temperatures and moisture contents at 6 hours as the initial conditions. Therefore the discussion and analysis of the simulation results of abrupt and smooth boundary conditions from time zero are judged to be of interest. The analysis of these different boundary conditions are hence continued in the paper.

Simulated temperature and moisture content profiles from *test 2*, during a period up to 72 hours, are shown in Fig. 3.

The initial moisture content and the temperature parameters differed between tests 1 and 2. The temperature gradient however approximated 34°C/m.

Calculated temperatures at 72 hours, in test 2, followed the measured values closely. A low initial moisture content, as in test 2, results however in a lower thermal diffusivity than that of test 1. The lower thermal diffusivity seemed to be under-estimated because the cooling in the simulation of test 2 was less than measured near the start of the test. The results were the same irrespective of how the cold end boundary condition was imposed.

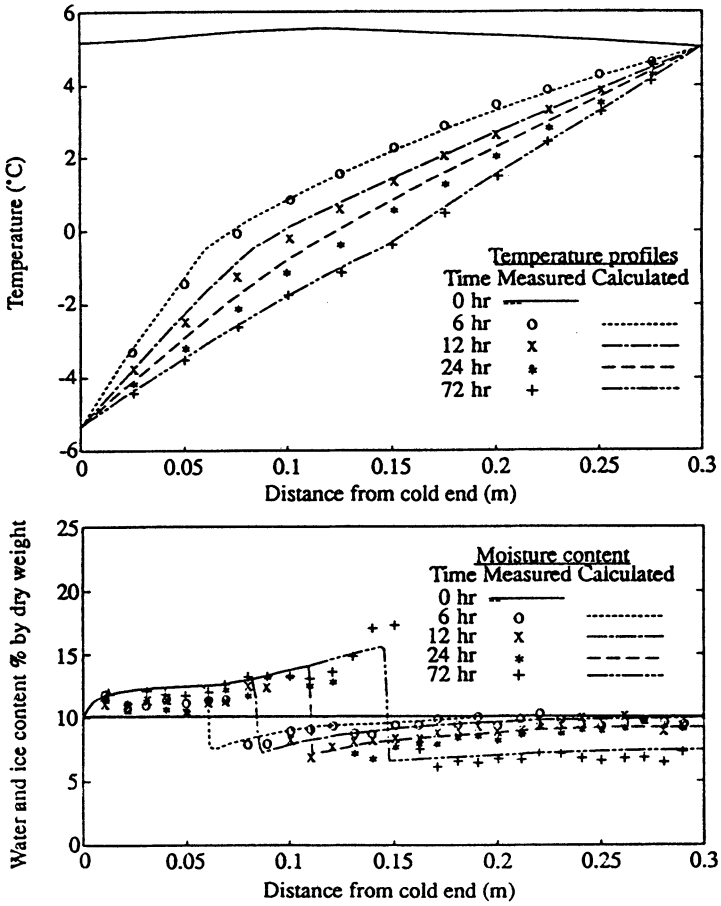

Fig. 3. Experimental data and simulation results of test 2, showing temperature and moisture content profiles.

The calculated moisture content profiles described in Fig. 3 were similar to the measured profiles with discrepancies of less than 2%, except at the frost front positions. Calculated frost fronts occurred about 0.005-0.02 m before measured.

The low initial moisture content also influenced the water diffusivity. The moisture accumulation in the frozen zone during test 2 was slightly over-estimated compared with measured values. This did not occur during the simulation of test 1. One explanation for this difference may be that a lower initial water content reduced ice formation. Since the water diffusivity, due to ice content, was limited by an impedence factor, the water diffusivity in the frozen zone was greater during test 2 than test 1. Hence, the range of the water diffusivity parameters, from low to high water/ice contents, seems to be important when simulating amounts of water accumulation.

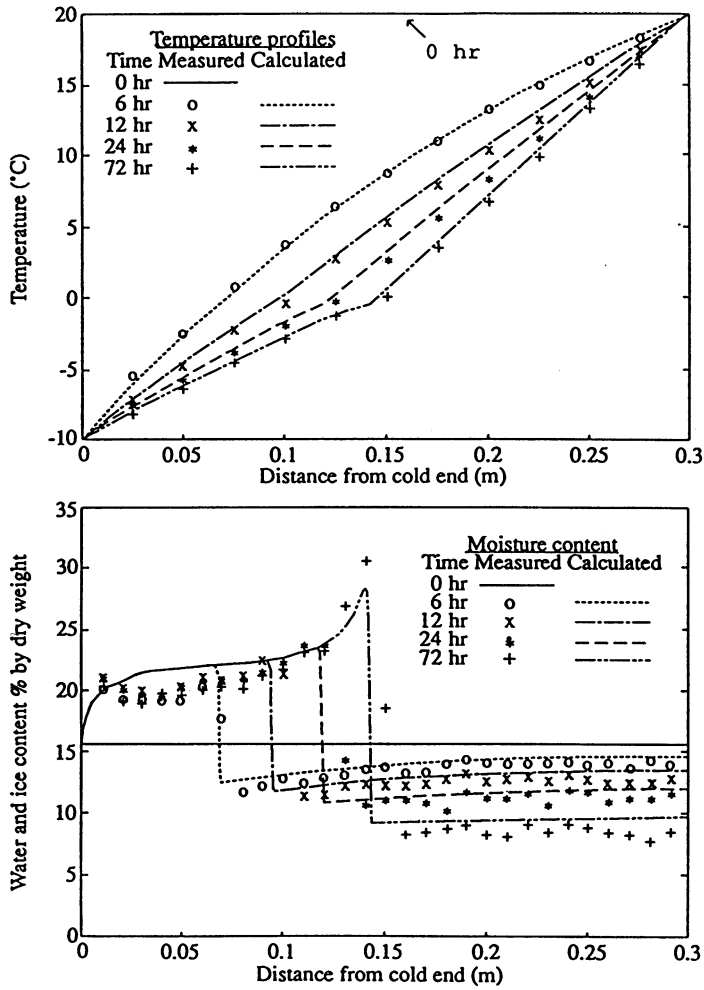

Fig. 4. Experimental data and simulation results of test 3, showing temperature and moisture content profiles.

Similarly to test 1, the total water accumulation closest to the cold end was about 12 % during a smooth temperature boundary condition, compared to 10 % when the abrupt boundary condition was used. At positions ahead z = 0.01 m, the moisture profiles were approximately the same as the results presented in Fig. 2. No differences between the frost front positions during abrupt and smooth boundary conditions in the simulations of test 2 were evident.

Simulated temperature and moisture content profiles from *test 3*, during a period up to 72 hours, are shown in Fig. 4. The temperature gradient was 100°C/m in the column.

The calculated temperature profiles in Fig. 4 followed the measured values closely.

A simulation with a smooth time-temperature boundary condition resulted in a total moisture content of about 24 % at the cold end boundary. At a distance of about 0.015 m from the cold end, the moisture contents were the same as the results presented in Fig. 4. At a distance of 0.015 m to approximately 0.10 m, the moisture contents were 0-0.7 % closer to measured values. Hence, the abrupt temperature boundary condition seemed to produce too large a water accumulation near the start of the experiment. A faster frost front penetration of 0.002 m and a lower temperature profile of about −0.3°C at 6 hours also resulted. There was however no difference in the frost front positions, during different temperature boundary conditions at 12, 24 and 72 hours.

Note that the frost fronts were at temperatures less than 0°C in Figs. 2-4. The explanation of this is that a freezing-point depression was necessary before ice could form with available water content, *i.e.* to satisfy Eq. (4). The initial moisture contents in combination with the imposed temperature gradients hence determined the frost front positions.

The following conclusions are evident from the results obtained with abrupt and smooth time-temperature boundary conditions and different initial moisture contents. The final frost front positions, *i.e.* the vertical elements of the total moisture contents curves in Figs. 2-4, are not sensitive to time-dependent temperature boundary conditions.

The frost depths and associated total accumulated moisture contents are determined by the minimum prevailing temperatures and the initial moisture contents before freezing. That is provided that no water is added to, or removed from, the system.

A Freezing and Thawing Cycle

The validation results of the model were acceptable for the freezing process. This is concluded on basis of the obtained relatively small discrepancies between simulated and measured values in regard to the unknown accuracy of the estimated (*e.g.* see Jame and Norum 1980) water and thermal diffusivity coefficients for different frozen conditions. No similar laboratory experiments examining the thawing process are however available for further validation. Results from a freezing and thawing cycle, simulated with the present model, will therefore be discussed qualitatively.

The freezing and thawing cycle in this study was governed by a heat flux at one end of a horizontal soil column and zero heat flux at the other end. The heat flux, Q, varied with a periodic sinusoidal function according to

$$Q \equiv 100 \sin(2\pi \text{ time}/72) \text{ [W/m}^2\text{]} \quad (10)$$

This resulted in a freezing process during the first 36 hours and thawing during the following 36 hours.

The total water content of the soil column was constant *i.e.* zero flux at the boundaries. The initial conditions are displayed in Fig. 5 as the profiles at time zero. The porous media characteristics were the same as those described in freezing tests conducted by Jame (1977). For the current qualitative study a 5-second time interval and a 0.0025 m space-increment were chosen. Energy and mass were conserved during the simulation.

The temperature, ice content and water content profiles of the freezing and thawing cycle are shown in Fig. 5.

Ice Content – A study of the ice contents on freezing (Fig. 5c) indicates that the main ice growth at the cold end of the column was within 14.4 hours (about 70 % within 7.2 hours).

The thawing of ice started slowly after the temperature minimum, *i.e.* before 36 hours. The melt was faster (Fig. 5d) as soon as the boundary flux brought heat into the soil column. A melt front was established between 43.2 and 50.4 hours and an ice zone remained. The melt front was defined by the partition between the ice-free zone with a temperature above 0°C and the ice zone, where temperature was below 0°C. It should be noted that the ice growth still continued at the cold front in the mid part of the soil column. This was because a very small temperature gradient, 0.01°C/m, still existed ahead of the high ice content region. Bulges on the ice content curves on the side towards the flux boundary occurred at 50.4, 57.6 and 64.8 hours. These bulges corresponded to a more saturated local pore space than surrounding areas.

Water content – The water content decreased as soon as ice was formed. This affected the magnitudes of the diffusivity coefficient and the moisture gradient. Therefore, the mass transfer was towards the freezing front with its lower water content values and hence the water content decreased ahead of the cold front.

The unfrozen water contents increased by the corresponding melted content, as soon as melting of ice started at the boundary. This immediately created a moisture gradient, resulting in water movement towards the ice zone which had a lower water content. Consequently, in the melt zone, the direction of the water movement was from the melt front towards the zone with maximum ice content. The water movement ahead of the ice body, in the unfrozen zone, progressed towards the cold front during thawing, but this was less pronounced than during the freezing part of the heat flux cycle.

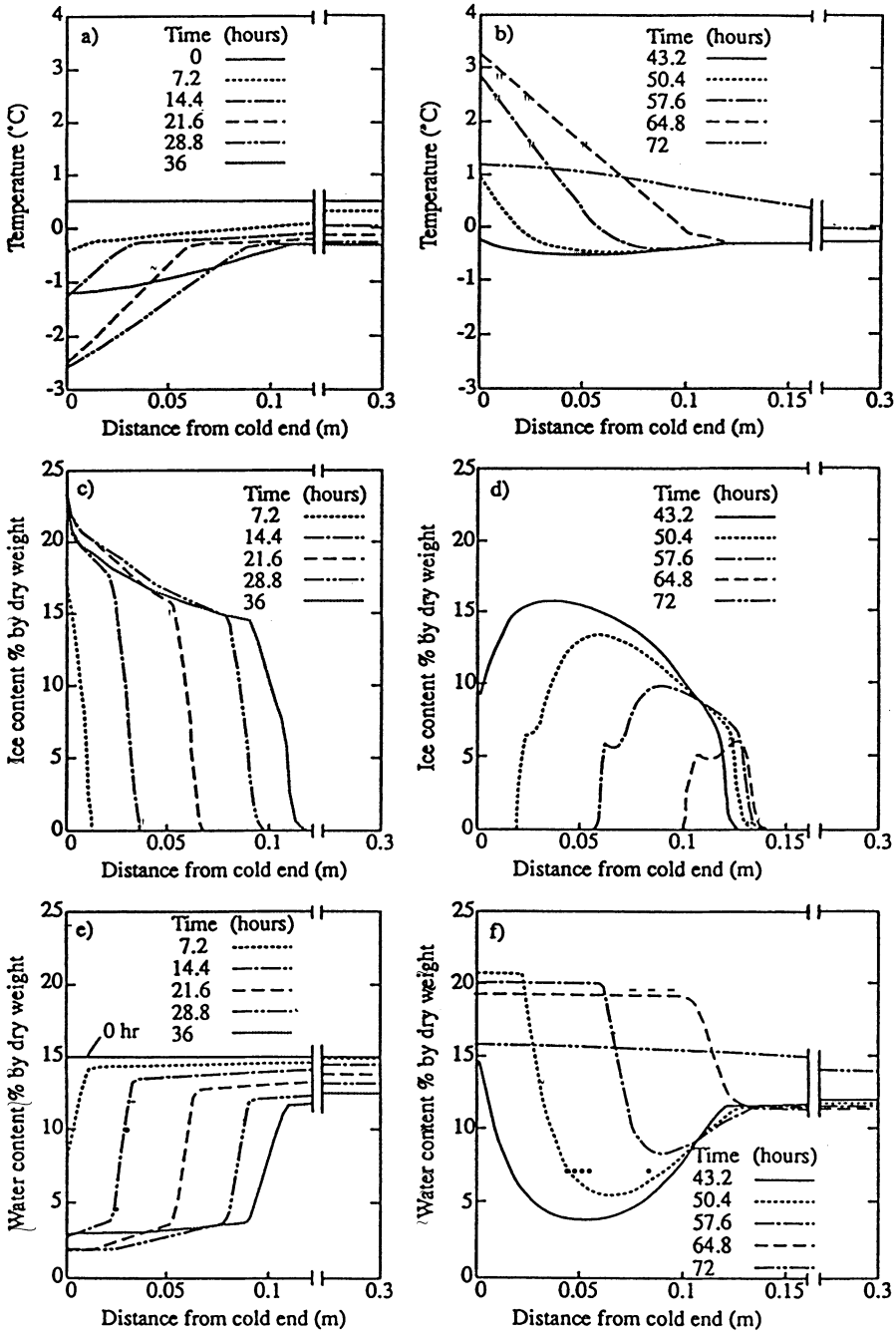

Fig. 5. Simulated temperature (a,b), ice content (c,d) and water content (e,f) of a freezing-thawing cycle. Freezing 0-36 hours, a-c-e and thawing 43.2-72 hours, b-d-f.

Discussion

Validation

Simulations of the three tests with the proposed new method can be carried out with abrupt boundary conditions from time zero. Little difference between measured and calculated temperature and moisture content profiles resulted.

Jame and Norum (1980) tested the validity of a model proposed by Harlan (1973). They used SWFC and an apparent heat capacity concept in an iterative procedure for solving the heat and mass transfer equations. The main difference between the simulation results presented by Jame and Norum (1980) and the simulation results presented in this paper was the calculated total moisture content at the cold end.

Their simulations from time zero resulted in very large moisture contents at the cold end. These simulated values were about 30 % and 37 % in the same tests that have been simulated with our model, Figs. 2 and 4, respectively.

In the use of our model, simulations from time zero of these experiments did not result in such high accumulated moisture contents at the cold end. This was irrespective of how the cold end boundary condition was imposed, as a one-step change or as a smooth temperature time-dependence.

The difference of the results at the cold end, between the simulations with our model and the model as was tested by Jame and Norum (1980), shows that without any exact measurement of the moisture content at the cold end, no final conclusion about the real magnitude of the moisture content at the cold end can be drawn. No visual ice layer was however found directly under the cold plate at the end of each test by Jame (1977). This may indicate that the real moisture content at the cold end had to be closer to the measured values at 0.01 m than to those simulated by Jame and Norum (1980).

Freezing and Thawing

A supercooling of the pore water was needed before ice formation could begin. This was due to moderate initial moisture content. The water flow towards the freezing front caused the moisture content to decrease in the unfrozen part of the soil column. Lesser amounts of water in this part, then required even lower temperatures before ice formation could start.

During thawing, melt water was transported towards the ice zone. Ice was melting at the melt front, but at the adjacent positions, in the ice zone, there was a net outflux of heat towards the zone with higher ice contents. This may be explained by the high non-linear thermal parameters at the melt front and resulted in ice growth, locally in the melt zone. It is presently not clear if the locally increased ice content is an expected physical phenomena or only a result of the simplification and assumptions in the set of equations used. Ice growth also continued at the cold

side of the ice zone but this was caused by a very small, still acting freezing temperature.

The following conclusion is evident from the simulation results of the freezing and thawing cycle. Frost depths can not be detected with only temperature measurements. The freezing and thawing simulation for example indicated that the frost depth was about 0.13 m when determined by ice content, while the corresponding temperature profile indicated that the whole profile was frozen if any temperature between 0°C and −0.3°C was used as an indicator for frost depth.

Although, no comparisons with measurements were presented for the freezing and thawing cycle, the results obtained look physically plausible.

Conclusions

The following conclusions can be drawn.

- The new numerical method for handling the phase-change process of freezing and thawing soils is easy to understand and follow from a physical point of view. The method is unsensitive to abrupt temperature boundary conditions with respect to final frost front position and its total accumulated moisture content.
- The validation of the proposed new method of modelling freezing processes in laboratory columns resulted in similar simulated and experimental total water contents and temperatures.
- Simulation results of laboratory tests with different initial moisture contents, but similar freezing temperature gradients indicated the following. The ranges of the water and thermal diffusivity parameters from low to high water/ice contents are important when simulating amounts of water accumulation and frost front penetration, respectively.
- From the qualitative study of the freezing and thawing cycle the following was noted:

  The frost depth defined as ice depth penetrated to about half the column length for the typical case studied in this paper. Frost depth defined with a freezing temperature indicated that the whole profile was frozen when using any temperature between 0°C and −0.3°C as an indicator.

  Ice growth continued during thawing at the cold side of the ice zone.

  In the melt zone, the direction of the water movement was from the melt front towards the zone with maximum ice content.

Acknowledgements

The authors wish to express their appreciation to Professor Anders Sellgren for his valuable advice in the preparation of this paper. The work was partly supported by the Swedish Council for Building Research.

References

Ayers, A.D., and Campbell, R.B. (1951) Freezing point of water in a soil as related to salt and moisture contents of the soils, *Soil Sci., Vol. 72*, pp. 201-206.

Cary, J.W. (1987) A new method for calculating frost heave including solute effects, *Water Resour. Res., Vol. 23(8),* pp. 1620-1624.

Childs, E.C., and Collis-George, N. (1950) The permeability of porous materials, *Proc. Roy. Soc. A., Vol. 201,* pp. 392-405.

Engelmark, H. (1984) Infiltration in unsaturated frozen soil, *Nordic Hydrology, Vol. 15*, pp. 243-252.

Engelmark, H. (1986) Infiltration and run-off during the period of snowmelt – field observations and numerical simulations. Licentiate Thesis 1986:08L, Div. of Water Resources Engineering, Luleå University of Technology, Luleå, Sweden, Report Series A, No. 145 (in Swedish with English summary), 72 pp.

Engelmark, H. (1992) Porous media characteristics for modelling heat and mass transfer in frozen unsaturated soil. Internal Report, Div. of Water Resources Eng., Luleå University of Technology, Luleå, Sweden, 7 pp.

Guymon, G.L., Hromadka, T.V. II, and Berg, R.L. (1980) A one dimensional frost heave model based upon simulation of simultaneous heat and water flux, *Cold Regions Science and Technology, Vol. 3*, pp. 253-262.

Guymon, G.L., and Luthin, J.N. (1974) A coupled heat and moisture transport model for arctic soils, *Water Resources Research, Vol. 10(5),* pp. 995-1001.

Halldin, S., Grip, H., Jansson, P.E., and Lindgren, Å. (1980) Micrometeorology and hydrology of pine forest ecosystems. II) Theory and models, *Ecol. Bull., Vol. 32,* pp. 463-503.

Harlan, R.L. (1973) Analysis of coupled heat fluid transport in partially frozen soil, *Water Resour. Res., Vol. 9(5),* pp. 1314-1323.

Hromadka II, T.V., Guymon, G.L., and Berg, R.L. (1981) Some approaches to modeling phase change in freezing soils, *Cold Science and Technology, Vol. 4(2),* pp. 137-145.

Jame, Y.W. (1972) Temperature effects on phase composition of partially frozen soil. Master Thesis, University of Saskatchewan, Saskatoon, Canada, 110 pp.

Jame, Y.W. (1977) Heat and mass transfer in freezing unsaturated soil. Ph. D. Thesis, University of Saskatchewan, Saskatoon, Canada, 211 pp.

Jame, Y.W., and Norum, D.I. (1980) Heat and mass transfer in a freezing unsaturated porous medium, *Water Resources Research, Vol. 16(4)*, pp. 811-819.

Jansson, P.E., and Halldin, S. (1980) SOIL water and heat model. Technical description, Swedish Coniferous Forest Project., Tech. Rep. 26, Uppsala, 81 pp.

Jensen, K.H. (1983) Simulation of water flow in the unsaturated zone including the root zone. Institute of Hydrodynamics and Hydraulic Engineering, Technical University of Denmark, Series Paper No. 33, 259 pp.

Karvonen, T. (1988) A model for predicting the effect of drainage on soil moisture, soil temperature and crop yield, Helsinki Univ. of Technology, Laboratory of Hydrology and Water Resources Management. Rep. 1988/1, 231 pp.

Karvonen, T. (1989) A model for simulating freezing and thawing of unsaturated soils. VTT Symp., 1989(94), pp. 267-281.

Kung, S.K.J., and Steenhuis, T.S. (1986) Heat and moisture transfer in a partly frozen nonheaving soil, *Soil Sci. Soc. Am. J., Vol. 50*, pp. 1114-1122.

Motovilov, Yu.G. (1977) Numerical modelling of the infiltration of water into frozen soils, *Meteorologiya i Gidrologiya, Vol. (9),* pp. 67-75, UDC 556. (072+14).

Sheppard, Marsha I., Kay, B.D., and Lock, J.P.G. (1978) Development and testing of a computer model for heat and mass flow in freezing soils. Third International Conference on Permafrost, Proceedings, Vol 1, pp. 76-81.

Svensson, U. (1986) PROBE – An instruction manual. Oceanogr. Rep. 10, Swed. Met. and Hydr. Inst., Norrk., Sweden.

Taylor, G.S., and Luthin, J.N. (1976) Numeric results of coupled heat-mass flow during freezing and thawing. Proceedings, 2nd Conference on Soil Water Problems in Cold Regions, Edmonton, Alta., Sept. 1-2, pp. 155-172.

Taylor, G.S., and Luthin, J.N. (1978) A model for coupled heat and moisture transfer during soil freezing, *Canadian Geotechnical Journal, Vol. 15*, pp. 548-555.

First received: 30 September, 1992
Revised version received: 18 February, 1993
Accepted: 22 February, 1993

Address:
Division of Water Resources Engineering,
Luleå University of Technology,
S-951 87 Luleå,
Sweden.